Stability of Molecular Adhesion Mediated by Confined Polymer Repellers and Ligand-Receptor Bonds

Jizeng Wang[*], **Jin Qian**[*] **and Huajian Gao**[*,†]

Abstract: Experiments have shown that stable adhesion of a variety of animal cells on substrates prepared with precisely controlled ligand distribution can be formed only if the ligand spacing is below 58 nm. To explain this phenomenon, here we propose a confined polymer model to study the stability of molecular adhesion mediated by polymer repellers and ligand-receptor bonds. In this model, both repellers and binders are treated as wormlike chains confined in a nanoslit, and the stability of adhesion is considered as a competition between attractive interactions of ligand-receptor binding and repulsive forces due to the size mismatch between repellers and binders. The force on each ligand-receptor bond is calculated from the confined polymer model, and the classic model of Bell is used to describe the association/dissociation reactions of ligand-receptor bonds. The calculated equilibrium bond distribution shows that there exists a critical ligand density for stable adhesion, corresponding to a critical ligand spacing which agrees not only qualitatively but also quantitatively with the experimental observation. In the case of stable adhesion, the model predicts an equilibrium separation between adhesion surfaces below 60% of the contour length of the ligand-receptor bonds.

1 Introduction

Cell-matrix and cell-cell adhesion are regulated by receptors on the membrane of one cell interacting with ligands on the surface of a substrate or another cell. A tight control of such molecular adhesion is required by many cell functions. For example, it is known that fast transitions between adhesion and de-adhesion are of key importance to the behavior of leucocytes [1].

Living cells can regulate their adhesive interactions via different mechanisms. In integrin-mediated cell adhesion, Yauch et al. [2] showed that α^4 tail deletion exposes the β_1 cytoplasmic domain, leading to cytoskeletal associations that apparently restrict lateral diffusion of integrins and their accumulation into clusters, hence reduces adhesion. Similarly, Yap et al. [3] found that regulation of cadherin binding sites on cell surface by cadherin cytoplasmic tail is an important mechanism to modulate cell adhesion. In addition to such specific regulations of receptors [2, 3], experiments also showed that cell adhesion involves more complicated mechanisms than mere switching between active and inactive binding states. For example, it has been recognized that receptor-independent phenomena, such as repeller molecules on the cell surface, can regulate cell adhesion [4]. A prominent example is glycocalyx that is found on most leucocytes [5, 6]. In the review article by Vitte et al. [4], experimental data have been described to support the view that (i) cell adhesion is significantly influenced by glycocalyx and (ii) under physiological conditions, glycocalyx may be altered by physiological or pathological stimuli to regulate adhesion. It has been shown that endothelial cell activation by chemotactic oligopeptide fMet–Leu–Phe or ischemia can lead to release of glycocalyx compontents which enhance leukocyte capture and inflammation [7], and that phagocytic cells can modulate specific components of their glycocalyx to regulate their binding capacity [8].

An interesting phenomenon on receptor-independent adhesion has been reported by

[*] The Division of Engineering, Box D, Brown University, 182 Hope Street, Providence, RI 02912, USA

[†] Corresponding author. Tel.: +1 401 863 2626; Fax: +1 401 863 9025; E-mail: Huajian_Gao@Brown.edu

Spatz and co-workers [9, 10]. They have shown that stable focal adhesions on substrates prepared with precisely controlled ligand distribution can be formed only if the ligand spacing is below 58 nm and no adhesion is possible for ligand spacing above 73 nm, and these critical spacings seem to be insensitive to cell types [9]. A feasible explanation of this phenomenon has been provided by Lin et al. [11] by considering the competition between thermal fluctuations of cell membranes and ligand-receptor binding. However, whether the cell surface repellers such as glycocalyx can also play a role in this phenomenon has not been investigated. To stimulate further discussions on this issue, here we consider an alternative model of cell adhesion via opposing forces induced by polymer repellers and ligand-receptor bonds. In this model, we treat repellers and binders as worm-like chains confined in a nanoslit in which ligand-receptor bonds transit stochastically between open and closed states. It will be shown that there indeed exists a critical ligand spacing on the order of 58nm for stable molecular adhesion. In contrast to the membrane fluctuation model of Lin et al. [11], the present model provides an alternative explanation of the critical ligand spacing observed by Spatz et al. [9, 10]. In the case of stable adhesion, the model also predicts an equilibrium separation between the adhesion surfaces below 60% of the contour length of the ligand-receptor bonds.

2 Force-separation relation for a tethered polymer chain confined in a nanoslit

For a free polymer chain of contour length L and persistence length p, the mean-squared radius of gyration R_g^2 can be expressed as [12]:

$$R_g^2 = \frac{1}{3}Lp - p^2 + \frac{2p^3}{L} - \frac{2p^4}{L^2}(1 - e^{-L/p}). \tag{1}$$

When such a polymer chain is confined inside a nanoslit of separation h, a force f will be imposed on the opposing parallel walls. This force can be derived based on the free energy expression given

by Chen and Sullivan [13] as

$$f =$$
$$- \pi^2 R_g^2 k_B T \frac{2 + c_1(p/h) + c_2(p/h)^2}{6h^3[1 + c_3(p/h) + c_4(p/h)^2]^{5/3}} \tag{2}$$

where $c_1 = 2.64533$, $c_2 = 3.43067$, $c_3 = 1.984$, $c_4 = 5.146$. Eq. (2) shows a repulsive force when $h \ll L$. If the two ends of the polymer chain are tethered to the opposing walls of the slit, the force-separation relation can differ significantly from that in Eq. (2). In the limit of $h \to 0$, the effect of end tethering is expected to be small so that Eq. (2) should be approximately valid. In the opposite limit of $h \to L$, the chain becomes strongly stretched, and its force-separation relationship can be written, following Marko and Siggia [14], as

$$f = \frac{k_B T}{4p} \frac{1}{(1 - h/L)^2}. \tag{3}$$

For the intermediate range $0 < h < L$, we propose an interpolating formula on the force-separation relation:

$$f = \frac{k_B T}{p} \left[\frac{1}{4(1 - h/L)^2} - \frac{1}{4} - \frac{h}{2L} \right]$$
$$- \pi^2 R_g^2 k_B T \frac{2 + c_1(p/h) + c_2(p/h)^2}{6h^3[1 + c_3(p/h) + c_4(p/h)^2]^{5/3}}. \tag{4}$$

It can be easily verified that Eq. (4) matches the two limiting cases of Eqs. (2) and (3). We note that similar interpolation technique has been used by Marko and Siggia [14] to obtain the force-extension relation of an unconfined worm-like chain as

$$\frac{pf}{k_B T} = \frac{h}{L} + \frac{1}{4(1 - h/L)^2} - \frac{1}{4}, \tag{5}$$

where, in the absence of a confining slit, h represents the end-to-end distance of the chain.

Fig. 2 plots the force-separation/force-extension relations described by Eqs. (4) and (5). It can be seen from Fig. 2 that the force-separation relation of Eq. (4) differs fundamentally from the force-extension relation of Eq. (5). In Eq. (4), f depends on the ratio p/L and changes from attraction to repulsion when the slit separation h becomes sufficiently small.
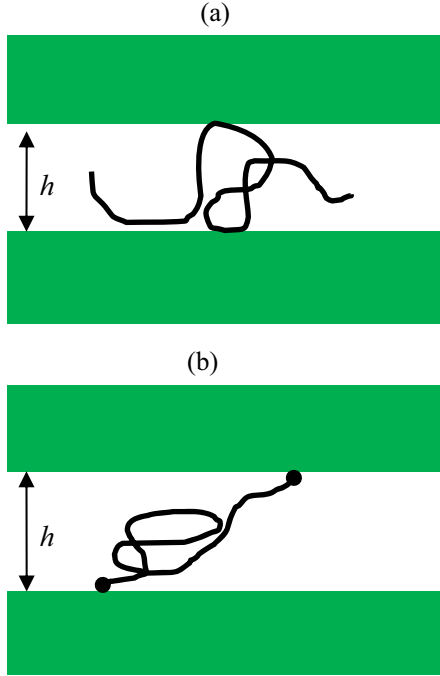
(a)

(b)

Figure 1: Schematic plot of a polymer chain confined in a nanoslit with (a) free (b) tethered ends. Lateral diffusion of the tethered chain ends is allowed.
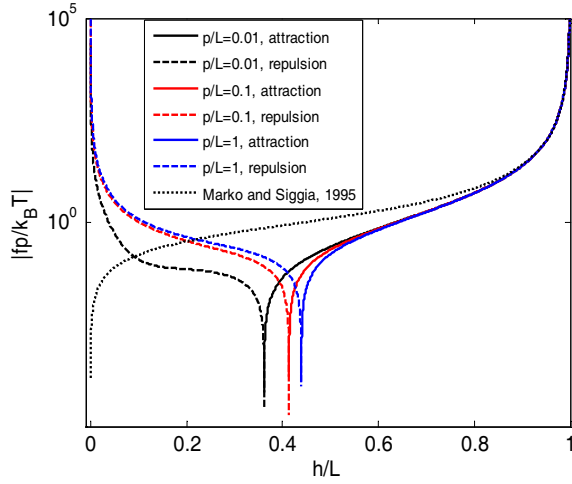

Figure 2: Comparison between the force-extension relation of an unconfined polymer chain, Eq. (5), and the force-separation relation of a confined chain with both ends tethered at the opposing walls of a nanoslit, Eq. (4).

3 Confined polymer model of molecular adhesion

As shown in Fig. 3, we consider molecular adhesion mediated by polymer repellers of density ρ_r
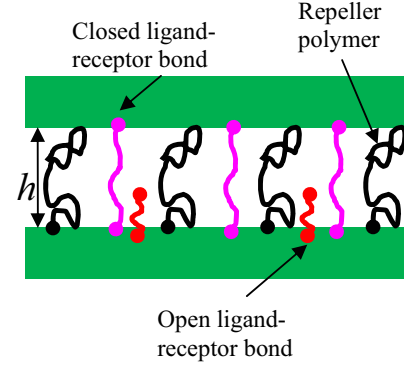

Figure 3: Schematic plot of confined polymer repellers and reactive ligand-receptor bonds. Note that both ends of a closed bond are tethered to the slit walls.

(number per unit area) and binders of density ρ_t. Among a total number of ρ_t ligand-receptor pairs per unit area, ρ_b of them are actually closed.

The ligand-receptor bonds are assumed to undergo reversible transitions between the open and closed states:

$$\mathbf{LR}^{\text{open}} \Leftrightarrow \mathbf{LR}^{\text{closed}}. \tag{6}$$

The kinetics of bond association/dissociation as a function of the force f on the bond can be described by the classic model of Bell [18] as,

$$\frac{d\rho_b}{d\tau} = \gamma(\rho_t - \rho_b) - \rho_b e^{f/F_b} \tag{7}$$

where $\tau = k_0 t$ is a normalized time, k_0 being the dissociation rate in the absence of a force, γ is the dimensionless rebinding rate, and $F_b = k_B T / x_b$, x_b being a measure of the distance between the minimum and the escape barrier of the binding potential. The force f in Eq. (7) can be obtained from Eq. (4) as

$$f = \frac{k_B T}{p_b} \left[\frac{1}{4(1 - h/L_b)^2} - \frac{1}{4} - \frac{h}{2L_b} \right]$$
$$- \pi^2 R_{gb}^2 k_B T \frac{2 + c_1(p_b/h) + c_2(p_b/h)^2}{6h^3 [1 + c_3(p_b/h) + c_4(p_b/h)^2]^{5/3}} \tag{8}$$

where L_b and p_b are the contour and persistence lengths of the closed bonds, and the mean-squared

radius of gyration R_{gb}^2 can be obtained from Eq. (1). We should note that the Bell model corresponds to the first order approximation of a one-step master equation in describing bond association/dissociation as discrete Markov events [15, 16].

At steady state, Eq. (7) becomes

$$\gamma(\rho_t - \rho_b) = \rho_b e^{f(h_{eq})/F}b. \tag{9}$$

According to Eq. (2), the repulsive stress of polymer repellers can be expressed as

$$\sigma_r = \rho_r \pi^2 R_{gr}^2 k_B T$$
$$\frac{2 + c_1(p_r/h_{eq}) + c_2(p_r/h_{eq})^2}{6h_{eq}^3[1 + c_3(p_r/h_{eq}) + c_4(p_r/h_{eq})^2]^{5/3}} \tag{10}$$

where L_r and p_r are contour and persistence lengths of the repellers, and the mean-squared radius of gyration R_{gr}^2 is given by Eq. (1). On the other hand, the attractive stress of closed ligand-receptor bonds is given by

$$\sigma_b = \rho_b \frac{k_B T}{p_b}\left[\frac{1}{4(1 - h_{eq}/L_b)^2} - \frac{1}{4} - \frac{h_{eq}}{2L_b}\right]$$
$$- \rho_b \pi^2 R_{gb}^2 k_B T$$
$$\cdot \frac{2 + c_1(p_b/h_{eq}) + c_2(p_b/h_{eq})^2}{6h_{eq}^3[1 + c_3(p_b/h_{eq}) + c_4(p_b/h_{eq})^2]^{5/3}} \tag{11}$$

according to Eq. (4). The repulsive and attractive forces must balance, i.e.

$$\sigma_b = \sigma_r. \tag{12}$$

It will be convenient to introduce the following dimensionless parameters

$$\rho = \frac{\rho_b}{\rho_t}, \quad z = \frac{h_{eq}}{L_b}, \quad \beta_1 = \frac{p_r}{L_b}, \quad \alpha_1 = \frac{p_b}{L_b},$$

$$\beta_2 = \frac{\pi^2 \rho_r R_{gr}^2 k_B T}{6L_b^3 \rho_t F_b}, \quad \sigma = \frac{\sigma_b}{\rho_t F_b} = \frac{\sigma_r}{\rho_t F_b},$$

$$\alpha_2 = \frac{\pi^2 R_{gb}^2 k_B T}{6L_b^3 F_b}, \quad \alpha_3 = \frac{k_B T}{p_b F_b}. \tag{13}$$

From Eq. (9), we have

$$\rho = \frac{\gamma}{\gamma + e^{\sigma/\rho}} \tag{14}$$

where we have used the relation $\sigma/\rho = f/F_b$. Now we can rewrite Eqs. (10, 11) as

$$\sigma = \beta_2 \frac{2z^2 + c_1\beta_1 z + c_2\beta_1^2}{(z^3 + c_3\beta_1 z^2 + c_4\beta_1^2 z)^{5/3}}, \tag{15}$$

$$\frac{\sigma}{\rho} = \alpha_3\left[\frac{1}{4(1 - z)^2} - \frac{1}{4} - \frac{z}{2}\right]$$
$$- \alpha_2 \frac{2z^2 + c_1\alpha_1 z + c_2\alpha_1^2}{(z^3 + c_3\alpha_1 z^2 + c_4\alpha_1^2 z)^{5/3}}, \tag{16}$$

and combine Eqs. (14 -16) into

$$\beta_2 \frac{2z^2 + c_1\beta_1 z + c_2\beta_1^2}{(z^3 + c_3\beta_1 z^2 + c_4\beta_1^2 z)^{5/3}}(\gamma + e^{\sigma/\rho})$$
$$= \gamma\alpha_3\left[\frac{1}{4(1 - z)^2} - \frac{1}{4} - \frac{z}{2}\right]$$
$$- \gamma\alpha_2 \frac{2z^2 + c_1\alpha_1 z + c_2\alpha_1^2}{(z^3 + c_3\alpha_1 z^2 + c_4\alpha_1^2 z)^{5/3}} \tag{17}$$

From Eqs. (14, 16, 17), we can calculate the normalized equilibrium density ρ of closed ligand-receptor bonds, the normalized interfacial stress σ and the normalized equilibrium separation z of the two surfaces.

4   Results and discussions

4.1 $\rho_r = 0$

In the case of $\rho_r = 0$, Eqs. (14, 16, 17) become

$$\rho = \frac{\gamma}{\gamma + e^{\sigma/\rho}}, \tag{18}$$

$$\frac{\sigma}{\rho} = \alpha_3\left[\frac{1}{4(1 - z)^2} - \frac{1}{4} - \frac{z}{2}\right]$$
$$- \alpha_2 \frac{2z^2 + c_1\alpha_1 z + c_2\alpha_1^2}{(z^3 + c_3\alpha_1 z^2 + c_4\alpha_1^2 z)^{5/3}}, \tag{19}$$

$$\alpha_3\left[\frac{1}{4(1 - z)^2} - \frac{1}{4} - \frac{z}{2}\right] =$$
$$\alpha_2 \frac{2z^2 + c_1\alpha_1 z + c_2\alpha_1^2}{(z^3 + c_3\alpha_1 z^2 + c_4\alpha_1^2 z)^{5/3}}. \tag{20}$$

In this case, it can be seen that the initial density of ligand-receptor bonds ρ_t does not play any role in

the stability of adhesion. It is not clear if the thermal fluctuation of membrane, as studied by Lin et al. [11], would be sufficient to destabilize adhesion even in the absence of any polymer repellers. Further experiments will be needed to clarify this issue.
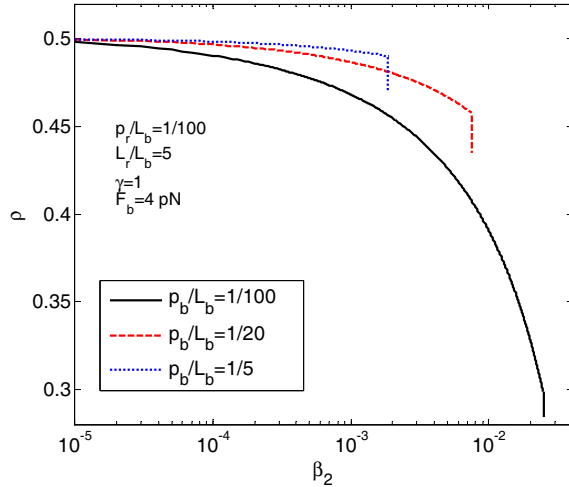

Figure 4: The normalized density of closed bonds as a function of the dimensionless parameter β_2 which scales in quadratic proportion to the ligand spacing.

4.2 $\rho_r \neq 0$

In cell adhesion, a common type of polymer repellers is glycocalyx, one kind of which has the contour length around $1\mu m$, the persistence length about $0.6nm$, and the number density on the order of several thousand per square micrometers [19]. For typical values, take $p_r/L_b = 1/100$, $L_r/L_b = 5$, $\gamma = 1$ and $F_b = 4pN$ in numerically solving Eqs. (14, 16, 17). Fig. 4 illustrates the normalized density of closed bonds as a function of dimensionless parameter β_2 under different ratios of p_b/L_b. It can be seen from Fig. 4 that the adhesion would fail when β_2 ($\propto 1/\rho_t$) exceeds a critical value. Fig. 5 shows that the equilibrium separation h_{eq} is always smaller than $0.6L_b$ and larger than $0.1L_b$.

For further discussions, we take $\rho_r = 3000/\mu m^2$ and, for a typical ligand-receptor pair, we consider binding between activated $\alpha_5\beta_1$ integrin
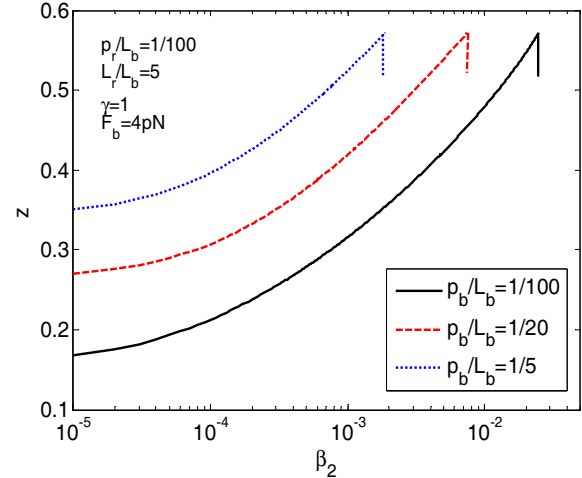

Figure 5: The normalized equilibrium separation as a function of the dimensionless parameter β_2 which scales in quadratic proportion to the ligand spacing.
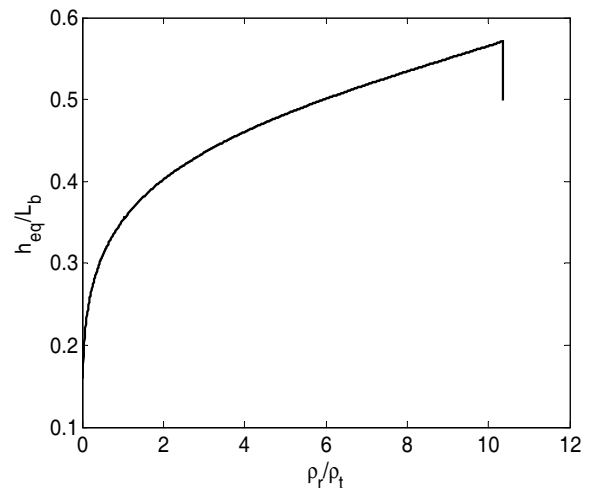

Figure 6: Dependence of the normalized equilibrium separation h_{eq}/L_b on the repeller-to-binder density ratio ρ_r/ρ_t.

to fibronectin, for which recent single molecule experiments have shown parameter values of k_0=0.012 Hz and $F_b \approx 9pN$, corresponding to $U_b \approx 24k_BT$. The rebinding rate can be estimated to be around $\gamma = 0.2$. The closed bond of activated $\alpha_5\beta_1$ integrin binding to fibronectin has a contour length of 62 nm and a persistence length of 0.4 nm [19, 20].

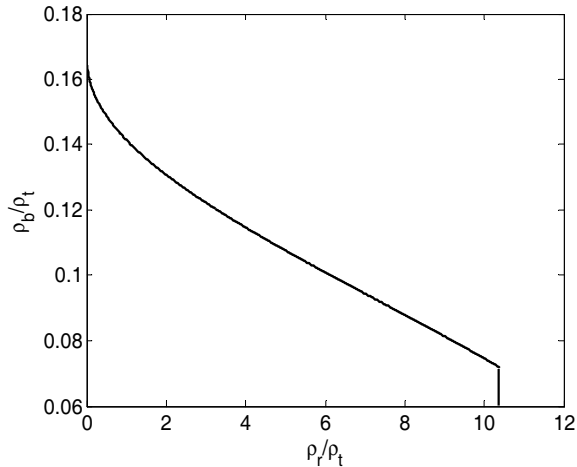Using the above parameters, Figs. 6 and 7 show

Figure 7: Dependence of the normalized equilibrium density of closed bonds ρ_b/ρ_t on the repeller-to-binder density ratio ρ_r/ρ_t.

that there exists a critical initial bond density of $288/\mu m^2$, corresponding to a critical ligand spacing of about 59 nm, which is very close to the experimentally observed critical spacing [9, 10]. In other words, it requires a minimum ligand density to stabilize molecular adhesion against non-specific repulsive forces due to glycocalyx. These results indicate that polymer repellers can play a significant role in the stability of cell adhesion and their effect can potentially explain the phenomenon of critical ligand spacing in cell adhesion.

5   Conclusions

We have established a simple model based on the behaviors of confined polymers to explain the experimental observation by Spatz and co-workers [9, 10] on the existence of a critical ligand spacing for stable cell adhesion. The point of view advocated in this model is that the competition between attractive forces due to ligand-receptor interaction and non-specific repulsive forces due to polymer repellers can play a significant or dominant role in cell adhesion. In the analysis, we have proposed a stress-separation relation for tethered polymer chains inside a nanoslit to estimate competing forces due to polymer repellers and ligand-receptor interactions. The clas-

sic model of Bell [18] has been used to describe the association/dissociation reactions of ligand-receptor bonds. Calculations based on this model provided an explanation of the experimental observation [9,10] that there exists a minimum ligand density for stable cell adhesion, corresponding to a critical ligand spacing which seem to agree not only qualitatively but also quantitatively with experiments.

In contrast to the membrane fluctuation model of Lin et al. [11], our model has focused on the critical conditions under which molecular adhesion can be stabilized against the non-specific repulsive forces of glycocalyx. It seems that both the membrane fluctuation model of Lin et al. [11] and the present model can quantitatively explain the observed critical ligand spacing, indicating considerable uncertainties in model building as well as parameter selections in this area of research. Further experiments will definitely be needed to fully resolve the issues involved.

References

1. Springer, T. A. (1990) *Annu. Rev. Cell Biol.* **6**, 359.

2. Yauch, R. L., Felsenfeld, D. P., Kraeft, S. K., Chen, L. B., Sheetz, M. P. & Hemler, M. E. (1997) *J. Exp. Med.* **186**, 1347.

3. Yap A. S., Brieher, W. M., Pruschy, M. & Gumbiner, B. M. (1997) *Curr. Biol.* **7**, 308.

4. Vitte, J., Benoliel, A., Pierres, A. & Bongrand, P. (2005) *Clinical Hemorheology and Microcirculation* **33**, 167.

5. Remold O'Donnell, E., Kennye, D. M., Parkman, R., Cairns, L., Savage, B. & Rosen, F. S. (1984) *J. Exp. Med.* **159**, 1705.

6. Cyster, J. G., Shotton, D. M. & Williams, A. F. (1991) *EMBO J.* **10**, 893.

7. Mulivor, A. W. & Lipowsky, H. H. (2004) *American Journal of Physiology-Heart and Circulatory Physiology* **286**, H1672.

8. Sabri, S., Soler, M., Foa, C., Pierres, A., Benoliel, A. & Bongrand, P. (2000) *J. Cell Sci.* **113**, 1589.

9. Arnold, M., Cavalcanti-Adam, E., Glass, R., Bluemmel, J., Eck, W., Kantlehner, M., Kessler, H. & Spatz, J. P. (2004) *ChemPhysChem* **5**, 383.

10. Spatz, J. P., Mossmer, S., Hartmann, C., Moller, M., Herzog, T., Krieger, M., Boyen, H. G., Ziemann, P. & Kabius, B. (2000) *Langmuir* **16,** 407.

11. Lin, Y., Inamdar, M. & Freund, L. B. (2008) *J. Mech. Phys. Solids*, **56**, 241.

12. Yamakawa, H. (1997) *Helical Wormlike Chains in Polymer Solutions* (Springer, Berlin).

13. Chen, J. Z. Y. & Sullivan, D. E. (2006) *Macromolecules* **39**, 7769.

14. Marko, J. F. & Siggia, E. D. (1995) *Macromolecules* **28**, 8759.

15. Erdmann, T. & Schwarz, U. S. (2004) *Phys. Rev. Letts.* **92**, 108102.

16. Erdmann, T. & Schwarz, U. S. (2004) *J. Chem. Phys.* **121**, 8997.

17. Qian, J., Wang, J. & Gao, H. (2008) *Langmuir*, DOI: 10.1021/la702401b.

18. Bell, G. I. (1978) *Science* **200**, 618.

19. Wang, J. & Gao, H. (2008) *J. Mech. Phys. Solids* **56**, 251.

20. Erdmann, T. & Schwartz, U. S. (2006) *Biophys. J.* **91**, L60.